Hindawi Publishing Corporation
Mathematical Problems in Engineering
Volume 2014, Article ID 407193, 10 pages
http://dx.doi.org/10.1155/2014/407193

Research Article

Fatigue Damage Assessment for Concrete Structures Using a Frequency-Domain Method

Hongyan Ding,[1,2,3] Qi Zhu,[3] and Puyang Zhang[1,2,3]

[1] *State Key Laboratory of Hydraulic Engineering Simulation and Safety, Tianjin University, Tianjin 300072, China*
[2] *Key Laboratory of Coast Civil Structure Safety, Tianjin University, Ministry of Education, Tianjin 300072, China*
[3] *School of Civil Engineering, Tianjin University, Tianjin 300072, China*

Correspondence should be addressed to Puyang Zhang; zpy_td@163.com

Received 22 October 2014; Revised 15 December 2014; Accepted 18 December 2014; Published 29 December 2014

Academic Editor: Yang Tang

A fatigue damage assessment for concrete was carried out according to Eurocode 2. Three frequency-domain methods, the level crossing counting (LCC) method, the range counting (RC) method, and a new proposed method, were used for the damage assessment. The applicability of these frequency-domain methods was evaluated by comparison with the rainflow counting method in the time domain. A preliminary numerical study was carried out to verify the applicability of the frequency-domain methods for stress processes with different bandwidths; thus, the applicability of the LCC method and the new method was preliminarily confirmed. The fatigue strength of concrete had a minor effect on the fatigue damage assessment. The applicability of the LCC and the new methods deteriorated for relatively low coefficients of variance of the stress process because the ultimate number of constant amplitude cycles was sensitive to the range of the cycles. The validity of the joint probability functions of the two methods was proven using a numerical simulation. The integration intervals of the two frequency-domain methods were varied to estimate the lower and upper bounds on the fatigue damage, which can serve as references to evaluate the accuracy of the time-domain method results.

1. Introduction

Fatigue is the process of gradual damage to materials that are subjected to continually changing stresses. Concrete fatigue is primarily a problem for offshore structures, railway sleepers, and bridges, which are often exposed to alternating loadings [1]. Unlike steel structures, both the range and level of stress affect fatigue damage in concrete structures [2]. In this study, the European Standard, Eurocode 2 [3], was applied to assess the fatigue damage of concrete structures.

A well-established procedure for fatigue damage assessment involves the time-domain analysis of the stress processes that a structure will be subjected to over its lifetime [4–6]. Stress processes in structures that are induced by wind, waves, or road irregularities often occur on a fairly irregular and random basis; however, only the ultimate number of stress cycles for a constant stress range and the mean stress that can be sustained up to failure is known. Thus, a description of the cycles in the stress records in terms of parameters such as the number of counted cycles, the distribution of cycle amplitudes, and the means is required. The counting method [7] was applied in this study. Level crossing counting (LCC), peak counting (PC), simple range counting (RC), and rainflow counting (RFC) are the counting methods most commonly used in engineering practice. The RFC method is widely accepted as the most efficient counting method available [8].

The fatigue damage of structures can also be assessed in the frequency domain. The frequency-domain method is faster and more cost efficient than the time-domain method [9–11]. Variations in parameters and optimization can be rapidly executed for a properly functioning frequency-domain method. The stress processes in the frequency domain are represented using a spectral formulation, such as a power spectral density (PSD) function, which provides information on the power distribution over a range of frequencies. The first n (typically 4) moments of the PSD function are used to find the probability density function (PDF) for the peaks and valleys of the stress process (i.e., the range of the stress and mean stress) [12]. The fatigue damage can be calculated by integration using the PDF and Palmgren-Miner's rule.

In this study, PDFs that are available in the literature and a PDF developed by the authors were applied to calculate the fatigue damage of concrete structures. The RFC method in the time domain is the standard method for fatigue assessment. The results of different frequency-domain methods were compared with the results of the RFC method to select the most effective frequency-domain methods. A preliminary numerical study was carried out to verify the applicability of the frequency-domain methods for stress processes with different bandwidths; thus, the applicability of the LCC method and the new method was preliminarily confirmed. The integration intervals of the two frequency-domain methods were varied to estimate the lower and upper bounds on the fatigue damage, which can serve as references to evaluate the accuracy of the time-domain method results. Few published reports on fatigue assessment for concrete in the frequency domain are currently available; thus, the results of this study can serve as a useful reference in this field [13].

2. Basic Theory

2.1. Frequency-Domain Process. A stress process $h(t)$ is assumed to be a stationary Gaussian process. The autocorrelation function of $h(t)$ is defined as follows [14]:

$$K(\tau) \equiv \overline{h(t)\,h(t+\tau)} = \lim_{T\to\infty} \frac{1}{2T}\int_{-T}^{T} h(t)\,h(t+\tau)\,d\tau. \quad (1)$$

The Fourier transform of the autocorrelation function is expressed as

$$K(\tau) = \int_{-\infty}^{\infty} S(f)\,e^{-i\omega\tau}df, \quad (2)$$

where the new function, $S(f)$, is the PSD of $h(t)$. $S(f)$ can also be written in terms of $K(\tau)$:

$$S(f) = \int_{-\infty}^{\infty} K(\tau)\,e^{i\omega\tau}d\tau. \quad (3)$$

Equations (2) and (3) are known as the Wiener-Khintchine relations.

We are typically not interested in distinguishing a PSD that is associated with a negative frequency from one that is associated with a positive frequency. A single-sided PSD can be defined as follows:

$$\overline{S(f)} = S(f) + S(-f) \quad (f \geq 0). \quad (4)$$

Variables that are encountered in engineering analysis, such as the stress, are real. The PSD is an even function for real variables; thus,

$$\overline{S(f)} = S(f) + S(-f) = 2S(f) \quad (f \geq 0). \quad (5)$$

The nth moment of the PSD function can be obtained from the characteristic of the PSD function. The spectral moments are defined as follows:

$$m_n = \int_0^{\infty} f^n \overline{S(f)}df. \quad (6)$$

The first four moments (m_0, m_1, m_2, and m_4) are the most commonly used moments of the PSD function.

The bandwidth of a signal is taken to be the frequency interval over which most of the signal power is concentrated. The bandwidth can be defined in terms of the spectral moments [15]:

$$\alpha_1 = \frac{m_1}{\sqrt{m_0 m_1}} \qquad \alpha_2 = \frac{m_2}{\sqrt{m_0 m_4}}$$
$$0 \leq \alpha_1, \quad \alpha_2 \leq 1. \quad (7)$$

These two bandwidth parameters tend to unity for a "narrow-band" signal and zero for a "wide-band" signal.

2.2. Fatigue Damage Assessment Method for Concrete Structures from Eurocode 2. In Eurocode 2, Palmgren-Miner's rule [16] is applied to calculate the total fatigue damage, as given in (8). A satisfactory fatigue resistance may be assumed for concrete under compression if $D \leq 1$:

$$D = \sum_{i=1}^{m} \frac{n_i}{N_i}, \quad (8)$$

where D is the total fatigue damage; m is the number of intervals with a constant amplitude; n_i is the actual number of constant-amplitude cycles in the interval "i"; N_i is the ultimate number of constant-amplitude cycles in the interval "i" that can be carried out before failure:

$$N_i = 10^{14((1-E_{\mathrm{cd,max},i})/\sqrt{1-R_i})} \qquad R_i = \frac{E_{\mathrm{cd,min},i}}{E_{\mathrm{cd,max},i}}$$
$$E_{\mathrm{cd,min},i} = \frac{\sigma_{\mathrm{cd,min},i}}{f_{\mathrm{cd,fat}}} \qquad E_{\mathrm{cd,max},i} = \frac{\sigma_{\mathrm{cd,max},i}}{f_{\mathrm{cd,fat}}}, \quad (9)$$

where R_i is the stress ratio; $E_{\mathrm{cd,min},i}$ is the minimum stress compression level; $E_{\mathrm{cd,max},i}$ is the maximum stress compression level; $\sigma_{\mathrm{cd,min},i}$ is the lowest stress in a cycle; $\sigma_{\mathrm{cd,max},i}$ is the highest stress in a cycle; and $f_{\mathrm{cd,fat}}$ is the design fatigue strength of the concrete. N_i is a function of both the peaks and valleys of the stress process.

2.3. Counting Methods. LCC, PC, RC, and RFC are the four most commonly used counting methods in engineering practice.

In the LCC method, every crossing of the predetermined stress levels is counted. Then, the most damaging level cycle is counted for fatigue by constructing the largest possible cycle, followed by the second largest cycle, and so on, until all of the level crossings have been considered.

In the PC method, the occurrence of a relative maximum or minimum stress value is identified. Peaks (valleys) that are above (below) the reference level are counted.

In the RC method, a range is defined as the difference between two successive reversals: the range is positive when a valley is followed by a peak and negative when a peak is followed by a valley.

The RFC method is the most frequently used cycle counting method in engineering practice. Starting from a local load maximum, Max_k, two minima are identified before and after Max_k, that is, Min_{k-} and Min_{k+}. The point with

the smallest deviation from Max_k is chosen as the rainflow minimum, $\mathrm{Min}_{k,\mathrm{RFC}}$, thus producing the kth rainflow cycle ($\mathrm{Min}_{k,\mathrm{RFC}}$, Max_k). The aforementioned procedure is repeated for the entire stress process.

3. Fatigue Damage Assessment for Concrete in the Frequency Domain

3.1. Joint Probability Density Applied to Fatigue Damage Assessment. As described in Section 2.2, N_i is a function of both the peaks and valleys in the stress process; thus, the fatigue damage for concrete structures is also a function of the peaks and valleys in the stress process. The joint probability density of the counted cycles $h(u, v)$, which is a function of peak "u" (corresponding to $\sigma_{\mathrm{cd,max},i}$ in (8)) and valley "v" (corresponding to $\sigma_{\mathrm{cd,min},i}$ in (8)), is constructed by applying the spectral moment parameters of the PSD function. As the RFC method is the "standard" counting method, we determine the joint probability density of counted cycles using $h_{\mathrm{RFC}}(u, v)$. However, no analytical solutions of $h_{\mathrm{RFC}}(u, v)$ are currently available, and only approximate approaches can be used to obtain an accurate fatigue damage assessment.

Tovo [17, 18] calculated the joint probability density of counted cycles for a zero-mean Gaussian process from the distribution of level crossing counted cycles as follows:

$$h_{\mathrm{LCC}}(u, v) = \begin{cases} \left[p_p(u) - p_v(u)\right]\delta(u+v) + p_v(u)\,\delta(u-v) & u \geq 0 \\ p_p(u)\,\delta(u-v) & u \leq 0, \end{cases} \tag{10}$$

where δ is the Dirac delta function and $p_p(u)$ and $p_v(u)$ are the cumulative distributions of the peaks and valleys, respectively:

$$p_p(x) = \Phi\left(\frac{x}{\sigma_x\sqrt{1-\alpha_2^2}}\right) - \alpha_2 e^{-x^2/2\sigma_x^2}\Phi\left(\frac{\alpha_2 x}{\sigma_x\sqrt{1-\alpha_2^2}}\right), \tag{11}$$

$$p_v(x) = p_p(-x), \tag{12}$$

where x is the stress, σ_x is the standard deviation, Φ is the cumulative Gaussian distribution, and α_2 is the bandwidth parameter, as defined by (7).

Tovo [17, 18] also calculated a joint probability density for the cycles in a Gaussian process, where the peaks and valleys distributions are given by (11) and (12), respectively, from the distribution of the counted cycles over the stress range:

$$h_{\mathrm{RC}}(u, v) = \frac{1}{\sigma_x^2\alpha_2^2 2\sqrt{2\pi}} \times e^{-(u^2+v^2)/4\sigma_x^2(1-\alpha_2^2)} e^{-((u-v)^2/4\sigma_x^2(1-\alpha_2^2))((1-\alpha_2^2)/2\sigma_x^2)} \times \left[\frac{u-v}{\sqrt{4\sigma_x^2(1-\alpha_2^2)}}\right]. \tag{13}$$

Equation (13) can be rewritten as a function of the mean stress "m" and stress range "s":

$$h_{\mathrm{RC}}(s, m) = \frac{1}{\sqrt{2\pi\sigma_x(1-\alpha_2^2)}} \times e^{-m^2/2\sigma_x(1-\alpha_2^2)} \frac{s}{\sigma_x\alpha_2^2} e^{-s^2/2\sigma_x\alpha_2^2} = p_m(m)\,p_s(s), \tag{14}$$

where $s = (u - v)/2$ and $m = (u + v)/2$.

Equation (14) shows that the joint probability density is a product of $p_m(m)$ and $p_s(s)$; thus, it is reasonable to assume that the mean stress "m" and stress range "s" are two independent variables. Then, other expressions for $p_s(s)$ can replace that in (14) to obtain a new joint probability density. The Dirlik method [19] is considered the most accurate approach for constructing an empirical expression for the PDF over the stress range "s" [20] and is used to obtain a new proposed $h_{\mathrm{NP}}(s, m)$:

$$h_{\mathrm{NP}}(s, m) = \frac{1}{\sqrt{2\pi\sigma_x(1-\alpha_2^2)}} e^{-m^2/(2\sigma_x(1-\alpha_2^2))} p_{\mathrm{Dirlik}}(s), \tag{15}$$

$$p_{\mathrm{Dirlik}}(s) = \frac{1}{\sqrt{\sigma_x}}\left[\frac{G_1}{Q}e^{-Z/Q} + \frac{G_2 Z}{R^2}e^{-Z^2/2R^2} + G_3 Z e^{-Z^2/2}\right], \tag{16}$$

$$Z = \frac{s}{\sqrt{\sigma_x}} \quad x_m = \frac{m_1}{m_0}\left(\frac{m_2}{m_4}\right)^{1/2}, \tag{17}$$

where

$$G_1 = \frac{2\left(x_m - \alpha_2^2\right)}{1+\alpha_2^2} \quad x_m = \frac{1-\alpha_2^2-G_1+G_1^2}{1-R}$$
$$Z = 1 - G_1 - G_2 \quad R = \frac{\alpha_2 - x_m - G_1^2}{1-\alpha_2-G_1+G_1^2} \tag{18}$$
$$Q = \frac{1.25\left(\alpha_2 - G_3 - G_2 R\right)}{G_1}.$$

3.2. Expressions for Fatigue Damage. In this section, (10), (14), and (15) are used to calculate the fatigue damage in the frequency domain.

The expected peak occurrence frequency υ_p is defined as [21]

$$\upsilon_p = \sqrt{\frac{m_4}{m_2}}. \tag{19}$$

The fatigue damage over a given time T can be calculated as follows:

$$E(D) = T\upsilon_p \iint \frac{h(u, v)}{N_i(u, v)}\,du\,dv. \tag{20}$$

When $h_{\mathrm{LCC}}(u, v)$ (see (10)) is used, the component related to $\delta(u - v)$ may be neglected in the calculation because this

function implies that $u = v$; that is, there is no effect on the damage. When $u \leq 0, h_{\mathrm{LCC}}(u, v) = p_p(u)\delta(u - v)$; thus,

$$\begin{aligned} E\left(D'\right) &= Tv_p \iint \frac{h(u,v)}{N_i(u,v)} du\, dv \\ &= Tv_p \iint \frac{p_p(u)\,\delta(u-v)}{N_i(u,v)} du\, dv \\ &= Tv_p \iint_{-\infty}^{0} \frac{p_p(u)\,\delta(u-v)}{N_i(u,v)} du\, dv \\ &= Tv_p \int_{-\infty}^{0} \left(\int_{-\infty}^{0} \frac{p_p(u)\,\delta(u-v)}{N_i(u,v)} du \right) dv \\ &= Tv_p \int_{-\infty}^{0} \frac{p_p(v)}{N_i(v,v)} dv. \end{aligned} \tag{21}$$

From the definition of N_i, $N_i(v, v) \to \infty$; thus, $E(D') \to 0$, and the component related to $\delta(u - v)$ clearly has no effect on the damage.

Equations (10)–(15) and (21) are all based on a zero-mean process; for a process with a non-zero-mean m_x, these equations can easily be modified using a variable shift. In this study, we perform a fatigue damage assessment for concrete under compression; thus, all of the stresses have the same sign (and are hereafter assumed to be positive). The following equations are given for a non-zero-mean process.

The fatigue damage can be calculated by applying $h_{\mathrm{LCC}}(u, v)$ as follows:

$$\begin{aligned} E\left(D^{\mathrm{LCC}}\right) &= Tv_p \iint \frac{h(u,v)}{N_i(u,v)} du\, dv \\ &= Tv_p \iint \Big(\left[p_p(u-m_x) - p_v(u-m_x) \right] \\ &\qquad \times \delta\left((u-m_x)+(v-m_x)\right) \\ &\qquad \times \left(N_i(u,v)\right)^{-1} \Big) du\, dv \\ &= Tv_p \int_{m_x}^{\infty} \Bigg(\int_{-\infty}^{u} \Big(p_p(u-m_x) - p_v(u-m_x) \\ &\qquad \times \delta\left(u+v-2m_x\right) \\ &\qquad \times \left(N_i(u,v)\right)^{-1} \Big) dv \Bigg) du \\ &= Tv_p \left(\int_{m_x}^{2m_x} \frac{p_p(u-m_x) - p_v(u-m_x)}{N_i(u, 2m_x - u)} du \right. \\ &\qquad \left. + \int_{2m_x}^{\infty} \frac{p_p(u-m_x) - p_v(u-m_x)}{N_i(u,0)} du \right). \end{aligned} \tag{22}$$

Because all of the stresses are positive, the lower limit of the valley is zero. When $(2m_x - u) \leq 0$, the valley of a cycle is set to zero.

Similarly, the fatigue damage $E(D^{\mathrm{RC}})$ can be calculated by the RC method, and $E(D^{\mathrm{NP}})$ can be calculated by the new method developed by the authors, that is, by applying (14), (15), and (23):

$$E(D) = Tv_p \iint \frac{h(s,m)}{N_i(s,m)} ds\, dm. \tag{23}$$

As the stress record is assumed to be Gaussian, almost all of the values will fall in the interval $(m_x - 5\sigma_x, m_x + 5\sigma_x)$; thus, the following integration intervals can be used to calculate $E(D^{\mathrm{RC}})$ and $E(D^{\mathrm{NP}})$: $m : (m_x - 5\sigma_x, m_x + 5\sigma_x)$, $s : (0, 5\sigma_x)$. (The upper bound on the integration interval for s is estimated as $s = ((m_x + 5\sigma_x) - (m_x - 5\sigma_x))/2$. For $(m_x - 5\sigma_x) < 0$, the lower bound on the integration interval is set to zero.)

4. Numerical Simulation

Numerical simulations were performed to investigate the applicability of the aforementioned frequency-domain methods. The fatigue damage was assessed using the time-domain method with RFC and Palmgren-Miner's rule to obtain the "standard" results. The accuracy of the results obtained from the frequency-domain methods was evaluated by comparison with the accuracy of these "standard" results.

The aforementioned joint PDFs were all constructed from spectral moments and bandwidth parameters. Preliminary numerical simulations were carried out to investigate the effect of the bandwidth parameters, particularly α_2, on the applicability of the frequency-domain methods. Some PSDs with simple shapes (see Figure 1) were applied in the simulation. The random stress processes that were used in the RFC methods in the time domain can be derived from these PSDs (see Figure 2) [22, 23].

The design fatigue strength of concrete, $f_{\mathrm{cd,fat}}$, was chosen as 19.1 MPa using Eurocode 2. A given mean value m_x of 5.0 MPa was used for all of the spectra and random processes. All of the spectra had the same m_0 of 1.0 MPa^2, which was equal to the variances σ_x^2 of the stress processes. The total simulation time was 1,000 s.

The results of the preliminary numerical simulations are shown in Figure 3. D^{LCC}, D^{RC}, D^{NP}, and D^{RFC} denote the fatigue damage that was calculated using the LCC method, RC method, the new method, and RFC method, respectively. The results of the three aforementioned frequency-domain methods were normalized by the results obtained using the RFC method in the time domain (the order of magnitude of the absolute fatigue damage was 10^{-9}). Figure 3 illustrates that both the LCC method and the new method yielded accurate estimates of the fatigue damage compared with the RFC method over the entire bandwidth of the stress process. Both the LCC method and the new method yielded conservative results, where the values of $D^{\mathrm{LCC}}/D^{\mathrm{RFC}}$ were between 2.0 and 12.0 and the values of $D^{\mathrm{NP}}/D^{\mathrm{RFC}}$ were between 2.0 and 18.2. Both of these methods should be used in engineering practice to obtain preliminary estimates of the fatigue damage in the initial design stage and parametric studies. The range method yielded poor estimates for most bandwidths, and more accurate results were obtained only when using higher α_2 values. The orders of magnitude of

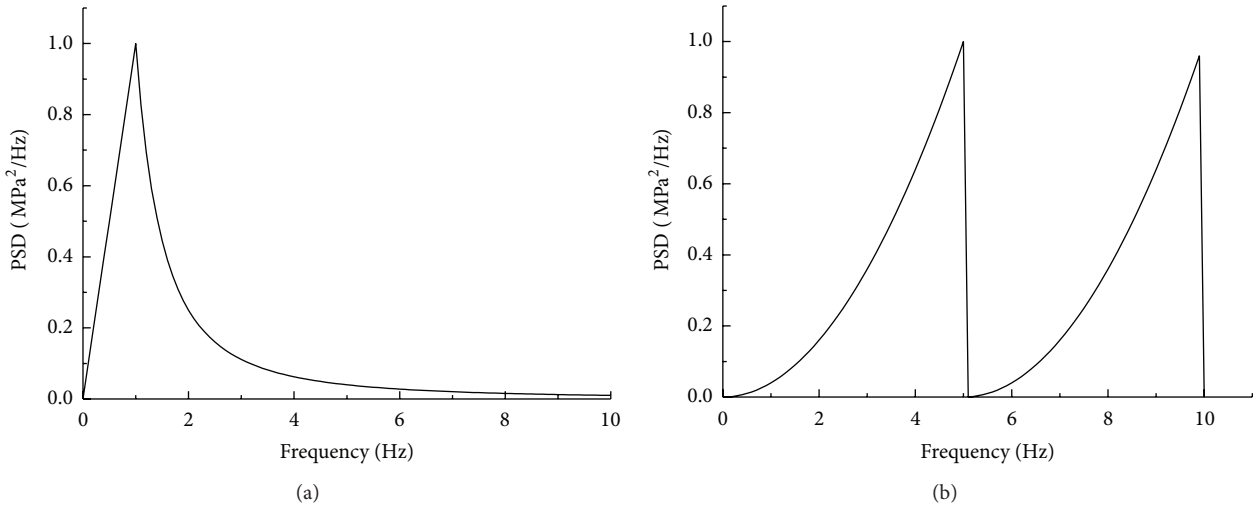

Figure 1: Examples of PSD curves.

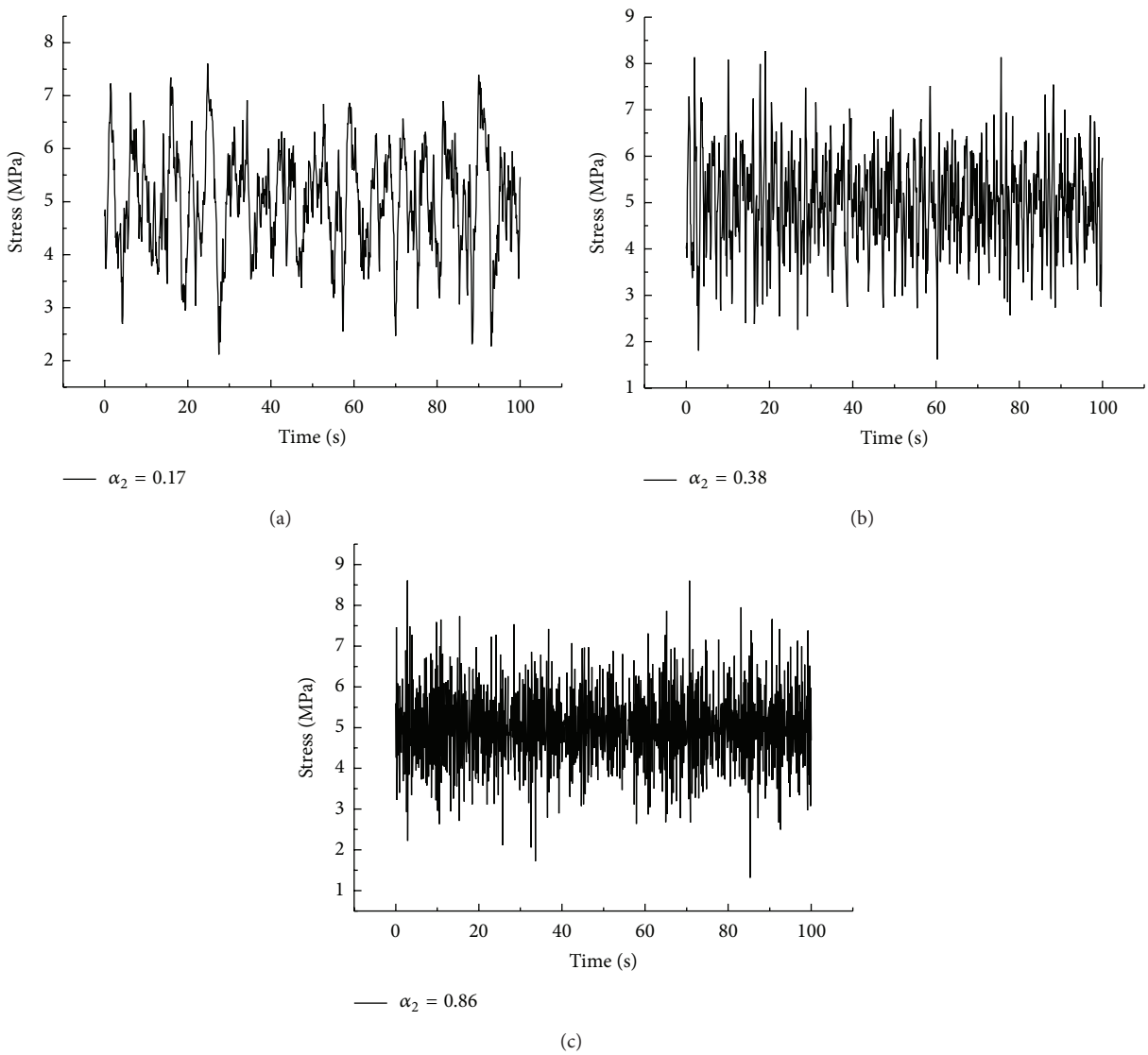

Figure 2: Examples of random processes with different bandwidth parameters.

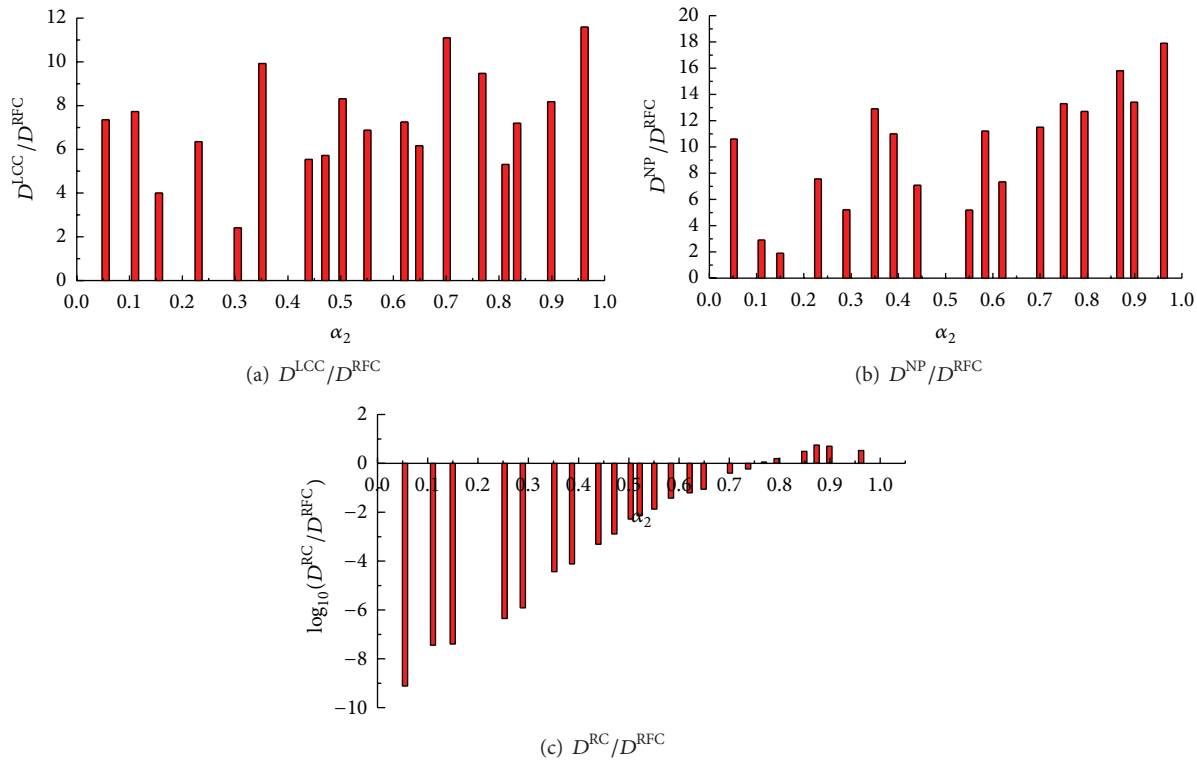

(a) D^{LCC}/D^{RFC} (b) D^{NP}/D^{RFC}

(c) D^{RC}/D^{RFC}

Figure 3: Results of the preliminary numerical simulations.

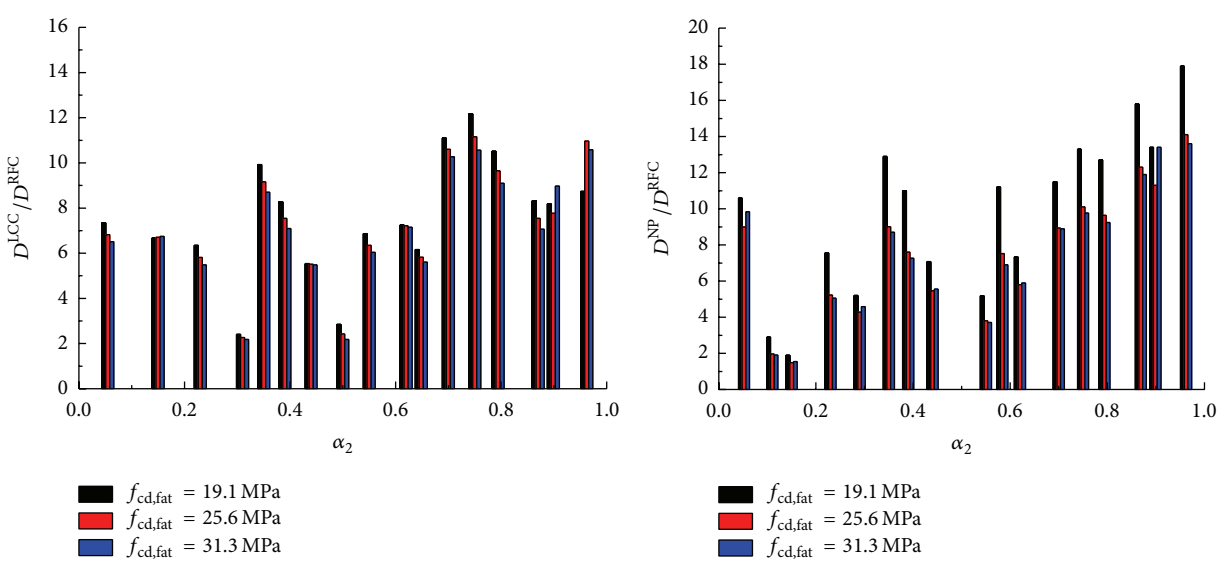

(a) D^{LCC}/D^{RFC} (b) D^{NP}/D^{RFC}

Figure 4: Effect of fatigue strength on fatigue damage.

D^{RC}/D^{RFC} were between 10^{-2} and 10^{-13} for values of α_2 below 0.65. The order of magnitude for D^{RC}/D^{RFC} approached unity when α_2 approached unity. Thus, the applicability of the RC method is limited to narrow-band stress processes.

We further verified the applicability of the LCC method and the new method by conducting parameter studies. First, the effect of the fatigue strength on the fatigue assessment was investigated for a stress process with a mean of m_x and a variance of σ_x^2. Fatigue strengths of 19.1, 25.6, and 31.3 MPa were considered. Figure 4 illustrates that, for these three different fatigue strengths, the values of D^{LCC}/D^{RFC} and D^{NP}/D^{RFC} were close to each other for all values of α_2: at

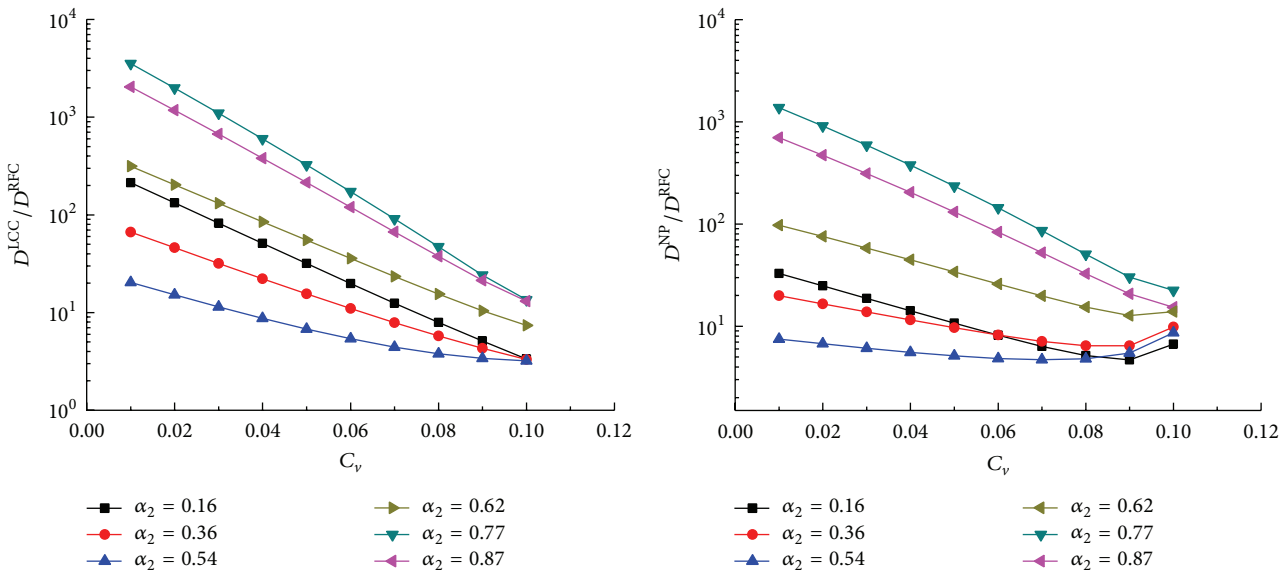

(a) D^{LCC}/D^{RFC} (b) D^{NP}/D^{RFC}

Figure 5: Effect of coefficient of variation on fatigue damage (in logarithmic scale).

some values of α_2, the three values were nearly equal to each other. Thus, the fatigue strength had only a minor effect on the values of D^{LCC}/D^{RFC} and D^{NP}/D^{RFC}.

The effects of the coefficient of variation $C_v = \sigma_x/m_x$ of the stress process on the applicability of these two methods were investigated for the same $I_m = m_x/f_{cd,fat}$ ratio, as shown in Figure 5. Similar D^{LCC}/D^{RFC} and D^{NP}/D^{RFC}curves were obtained for the same α_2 value. In some cases, the D^{LCC}/D^{RFC} and D^{NP}/D^{RFC} values increased dramatically as the coefficient of variation C_v decreased. Both the LCC method and the new method produced overly conservative estimates of the fatigue damage.

The applicability of the frequency methods deteriorated for lower coefficients of variation because N_i was defined as an exponential function. Figure 6 shows the cycle count versus the stress amplitude and the mean stress value of a specified stress record that were obtained using the RFC method and the corresponding fatigue damage caused by pairs of the stress amplitude and mean stress. Only a few cycles had stress amplitudes near the maximum amplitude, r_{max}, and a mean stress value near the mean values of stress range, m_x, whereas the corresponding fatigue damage was fairly high, with an order of magnitude that was nearly the same as that of the fatigue damage of the entire stress process. The value of N_i was highly sensitive to the potential maximum stress range of the cycle, and the total fatigue damage could be estimated by calculating the fatigue damage D^1 induced by 1 cycle with a pair of range and mean values of s_{max} and m_x, respectively (see (14)). As the stress record was assumed to be Gaussian, the limits of the stress interval $(m_x - n\sigma_x, m_x + n\sigma_x)$ were typically used as estimates of the upper and lower bounds, respectively, of the record; thus, it was reasonable to assume that s_{max} was equal to $n\sigma_x$. D^1 is defined as follows:

$$\begin{aligned} D^1 &= \frac{1}{N_i(s_{max}, m_x)} \\ &= 10^{-14((1-(m_x+s_{max})/f_{cd,fat})/\sqrt{1-(m_x-s_{max})/(m_x+s_{max})})} \\ &= 10^{-14((1-(m_x+n\sigma_x)/f_{cd,fat})/\sqrt{1-(m_x-n\sigma_x)/(m_x+n\sigma_x)})} \\ &= 10^{-14((1-(m_x+nC_v m_x)/f_{cd,fat})/\sqrt{1-(m_x-nC_v m_x)/(m_x+nC_v m_x)})} \\ &= 10^{-14((1-(1+nC_v)m_x/f_{cd,fat})/\sqrt{1-(1-nC_v)/(1+nC_v)})} \\ &= 10^{-14((1-(1+nC_v)I_m)/\sqrt{2nC_v/(1+nC_v)})}. \end{aligned} \tag{24}$$

The values of D^1 were calculated for $n = 2.0, 3.0, 3.1, 3.5, 4.0$, and 5.0 for different C_v values and a constant I_m. The ratios of $D^1(m_x, n\sigma_x)$ to $D^1(m_x, 3\sigma_x)$ are shown in Figure 7 (on a logarithmic scale). These ratios increased or decreased exponentially as C_v decreased for values of n that were greater or less than 3.0. The value of $D^1(m_x, 5\sigma_x)$ was approximately 9 orders of magnitude larger than $D^1(m_x, 3\sigma_x)$; that is, 1 cycle of stress with a pair of the stress range and the stress mean value of $(m_x, 5\sigma_x)$ produced the same damage as approximately 10^9 cycles of stress with a pair of the stress range and the stress mean value of $(m_x, 3\sigma_x)$. In the time domain, the number of cycles with high stress range could be counted as zero. In the frequency domain, the probability of the occurrence of the high stress range was relatively negligible but was a nonzero value, which had a tremendous effect when coupled to the damage that was induced by high stress range. Thus, the fatigue damage that was calculated using the

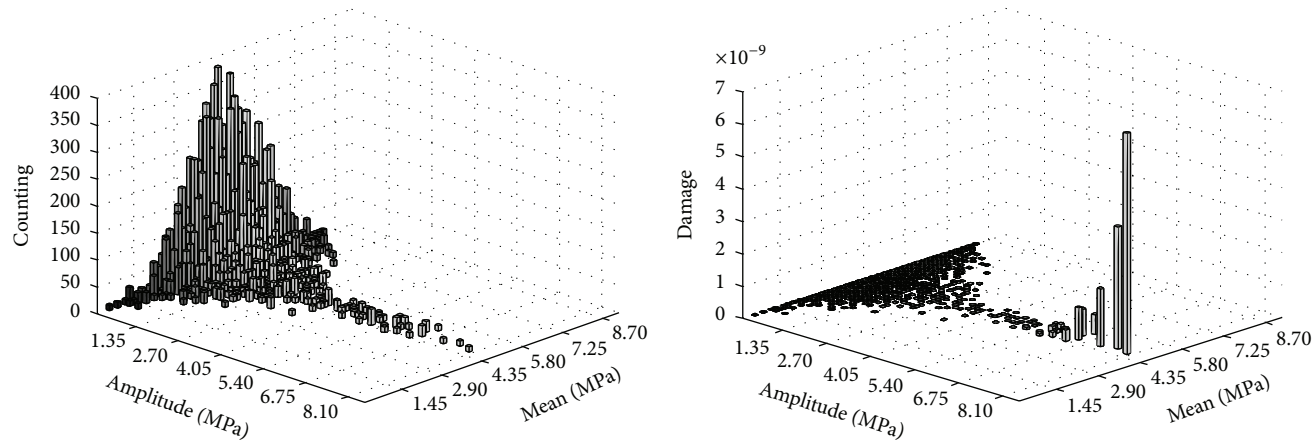

(a) Cycle count versus stress amplitude and mean stress value

(b) Corresponding fatigue damage

FIGURE 6: Cycle count versus stress amplitude and mean stress value and corresponding fatigue damage.

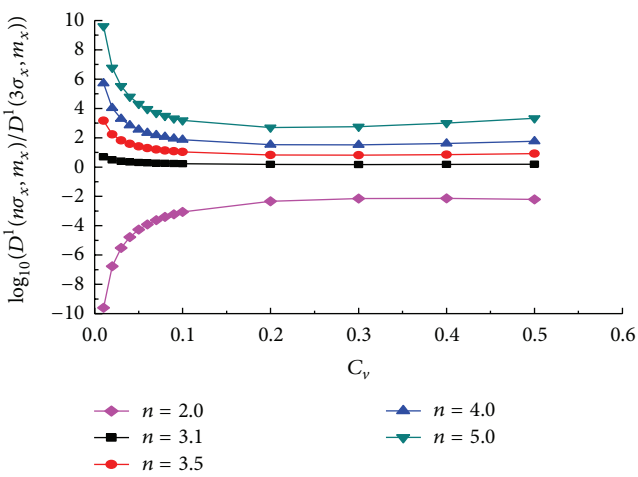

FIGURE 7: Ratios of $D^1(n\sigma_x, m_x)$ to $D^1(3\sigma_x, m_x)$ versus C_v.

frequency domain was larger than that calculated using the time domain.

We verified the applicability of these joint PDFs of the LCC method and the method for different C_v values by using an imaginary simple function $N_i = u \cdot v$ in the numerical simulation. Figure 8 shows the ratios of $D^{\mathrm{LCC}}/D^{\mathrm{RFC}}$ and $D^{\mathrm{NP}}/D^{\mathrm{RFC}}$ that were obtained. Both of these two ratios remained nearly constant for different C_v values when the value of N_i was not highly sensitive to the potential maximum stress ranges of the cycle. Both ratios were approximately 1.0. Thus, both of these two joint PDFs described the distributions of the "valleys" and "peaks" of the stress processes fairly accurately.

Different integration intervals were used for the LCC method and the new method to calculate the fatigue damage, which was normalized by the results of the RFC method (Figure 9). The effect of the integration intervals on the fatigue damage reflected the effect of the definition of N_i on the fatigue damage. The fatigue damage was overestimated using large intervals and underestimated using small intervals, where the extent of overestimation or underestimation was relatively higher for a lower C_v. As the joint PDFs described the "valleys" and "peaks" of stress processes fairly accurately, the upper and lower bounds on the fatigue damage can be estimated by varying the integration intervals in the frequency methods.

The RFC method in the time domain is generally considered the "standard" method for assessing fatigue damage; however, the stress process applied in the time-domain method is a fragment of the entire actual process. Stress processes with different maximum ranges may produce different fatigue damage assessments. Figure 10 shows a fatigue damage assessment on a logarithmic scale using 10 stress records, which had the same coefficients of variation because they were derived from the same PSD. The maximum fatigue damage was two orders of magnitude larger than the minimum fatigue damage. Thus, the RFC method in the time domain does not serve as an appropriate "standard" and should be used with caution; that is, different stress processes should be used in engineering practice. As noted above, varying the integration intervals in the two frequency-domain methods can be used to estimate the lower and upper bounds of the fatigue damage; thus, the results derived from the frequency-domain methods could serve as a reference to evaluate the accuracy of the results of the time-domain method.

5. Conclusion

Three frequency-domain methods were used for a fatigue damage assessment. The underlying principle of the frequency-domain method is the construction of a PDF for the "peaks" and "valleys" of the stress process (i.e., the stress range and mean stress). Two PDFs were taken from the literature, and one PDF was formulated by the authors. This novel PDF was constructed by replacing $p_s(s)$ in (14) using the Dirlik method (see (16)) and assuming that the stress range "s" and stress mean "m" were independent variables.

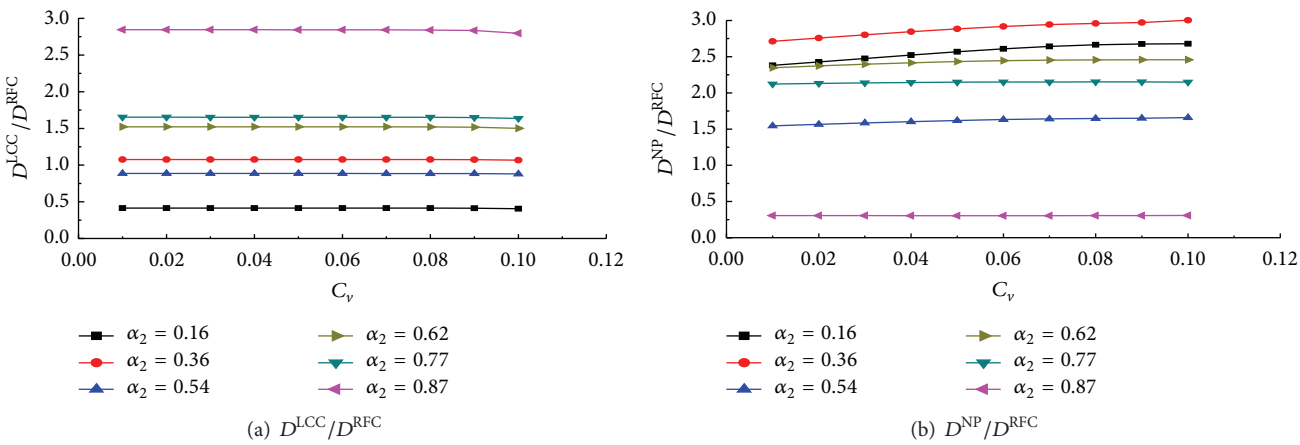

(a) D^{LCC}/D^{RFC} (b) D^{NP}/D^{RFC}

Figure 8: Applicability of two joint PDFs.

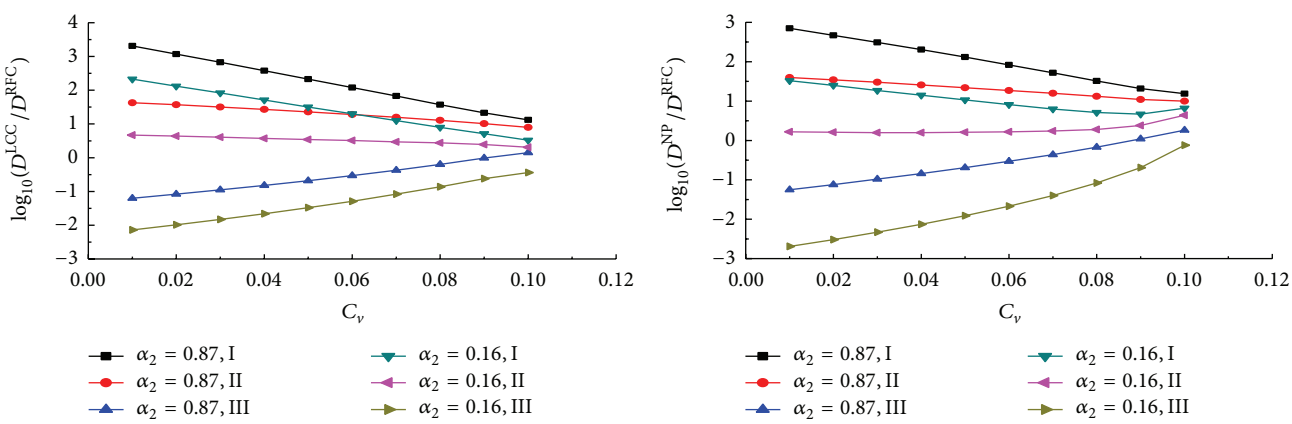

(a) Integration intervals for the LCC method, I: $s(-5\sigma_x, 5\sigma_x)$, $m(m_x - 5\sigma_x, m_x + 5\sigma_x)$, II: $s(-4\sigma_x, 4\sigma_x)$, $m(m_x - 4\sigma_x, m_x + 4\sigma_x)$, and III: $s(-3\sigma_x, 3\sigma_x)$, $m(m_x - 3\sigma_x, m_x + 3\sigma_x)$

(b) Integration intervals for the new method, I: $u(m_x, +\infty)$, II: $u(m_x, m_x + 4\sigma_x)$, and III: $u(m_x, m_x + 3\sigma_x)$

Figure 9: Effects of integration intervals on damage assessment.

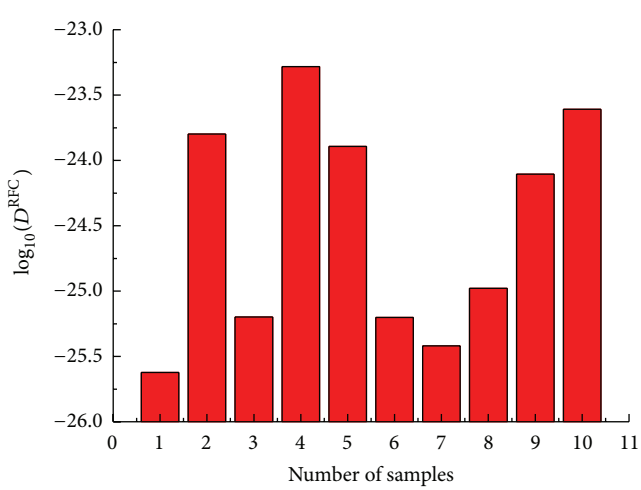

Figure 10: Fatigue damage assessment based on 10 stress records with the same parameters (e.g., α_1, α_2, m_x, σ_x).

The applicability of these three methods was investigated by comparing the results of the frequency-domain methods with those from the RFC method in the time domain. A preliminary study demonstrated that both the LCC method and the new method yielded accurate estimates over the entire range of bandwidths of the stress process, whereas the RC method yielded poor estimates for low bandwidths.

We carried out parametric studies to further verify the applicability of the LCC method and the new method. The fatigue strength of concrete had a slight impact on the applicability of these two methods. Decreasing the coefficient of variation deteriorated the applicability of these two methods for some cases. This behavior was attributed to the definition of N_i. The value of N_i was highly sensitive to the potential maximum stress ranges of the cycle, particularly for relatively low coefficients of variation. The validity of the two joint PDFs for the LCC method and the new method was evaluated by a numerical simulation. The integration intervals of the two

frequency-domain methods can be varied to calculate the lower and upper bounds on the fatigue damage, which can serve as references to evaluate the accuracy of the results of the time-domain method.

In conclusion, the RC method is only applicable to wide-band ($\alpha_2 > 0.65$) stress processes, and the LCC method and the new method are applicable for all bandwidths. Both the LCC method and the new method should be used in practical design for mutual authentication. Only pure compression was investigated in this study, and N_i was defined for pure tension and tension-compression [24, 25] as an exponential function, as in pure compression. Thus, the conclusions of this study are only applicable for the aforementioned cases.

Conflict of Interests

The authors declare that there is no conflict of interests regarding the publication of this paper.

Acknowledgments

The authors would like to acknowledge the support from the National Natural Science Foundation of China (Grant nos. 51379142 and 51309179), the International S&T Cooperation Program of China (Grant no. 2012DFA70490), and the Tianjin Municipal Natural Science Foundation (Grant no. 13JCYBJC19100).

References

[1] F. Göransson, *Fatigue assessment of concrete foundations for wind power plants [M.S. thesis]*, Chalmers University of Technology, Göteborg, Sweden, 2011.

[2] F. Olsson, *Fatigue assessment methods for reinforced concrete bridges in Eurocode [M.S. thesis]*, Chalmers University of Technology, Göteborg, Sweden, 2010.

[3] British Standards Institution, EN 1992-2:2005, Eurocode 2: Design of concrete structures. Concrete bridges. Design and detailing rules, 2005.

[4] H. Agerskov, "Fatigue in steel structures under random loading," *Journal of Constructional Steel Research*, vol. 53, no. 3, pp. 283–305, 2000.

[5] Z. Li, J. W. Ringsberg, and G. Storhaug, "Time-domain fatigue assessment of ship side-shell structures," *International Journal of Fatigue*, vol. 55, pp. 276–290, 2013.

[6] P. R. Thies, L. Johanning, V. Harnois, H. C. M. Smith, and D. N. Parish, "Mooring line fatigue damage evaluation for floating marine energy converters: Field measurements and prediction," *Renewable Energy*, vol. 63, pp. 133–144, 2014.

[7] S. Ariduru, *Fatigue life calculation by rainflow cycle counting method [M.S. thesis]*, Middle East Technical University, Ankara, Turkey, 2004.

[8] M. Matsuishi and T. Endo, *Fatigue of Metals Subjected to Varying Stress*, Japan Society of Mechanical Engineers, Fukuoka, Japan, 1968.

[9] X. Liu, G. Feng, and H. Ren, "Study on the application of spectral fatigue analysis," *Journal of Marine Science and Application*, vol. 5, no. 2, pp. 42–46, 2006.

[10] American Bureau of Shipping, *Spectral-Based Fatigue Analysis for Floating Offshore Structures*, 2005.

[11] G. Petrucci, M. Di Paola, and B. Zuccarello, "On the characterization of dynamic properties of random processes by spectral parameters," *Journal of Applied Mechanics*, vol. 67, no. 3, pp. 519–526, 2000.

[12] J. V. D. Tempel, *Design of support structures for offshore wind turbines [Ph.D. thesis]*, Delft University of Technology, Delft, The Netherlands, 2006.

[13] T. Kukkanen and T. P. J. Mikkola, "Fatigue assessment by spectral approach for the ISSC comparative study of the hatch cover bearing pad," *Marine Structures*, vol. 17, no. 1, pp. 75–90, 2004.

[14] P. Stoica and R. Moses, *Spectral Analysis of Signals*, Prentice Hall, 2005.

[15] M. Mršnik, J. Slavič, and M. Boltežar, "Frequency-domain methods for a vibration-fatigue-life estimation—application to real data," *International Journal of Fatigue*, vol. 47, pp. 8–17, 2013.

[16] M. Miner, "Cumulative damage in fatigue," *Journal of Applied Mechanics*, vol. 12, no. 3, pp. 159–164, 1945.

[17] R. Tovo, "Cycle distribution and fatigue damage under broad-band random loading," *International Journal of Fatigue*, vol. 24, no. 11, pp. 1137–1147, 2002.

[18] D. Benasciutti and R. Tovo, "Spectral methods for lifetime prediction under wide-band stationary random processes," *International Journal of Fatigue*, vol. 27, no. 8, pp. 867–877, 2005.

[19] T. Dirlik, *Applications of Computers in Fatigue Analysis*, University of Warwick, Coventry, UK, 1985.

[20] P. Ragan and L. Manuel, "Comparing estimates of wind turbine fatigue loads using time-domain and spectral methods," *Wind Engineering*, vol. 31, no. 2, pp. 83–99, 2007.

[21] J. M. Naser, *Analysis of vibration-induced fatigue cracking in steel bridges [M.S. thesis]*, Chalmers University of Technology, Göteborg, Sweden, 2010.

[22] M. Shinozuka and G. Deodatis, "Simulation of stochastic processes by spectral representation," *Applied Mechanics Reviews*, vol. 44, no. 4, pp. 191–204, 1991.

[23] B. Hu and W. Schiehlen, "On the simulation of stochastic processes by spectral representation," *Probabilistic Engineering Mechanics*, vol. 12, no. 2, pp. 105–113, 1997.

[24] Det Norske Veritas, DNV-OS-C502, Offshore concrete structures, 2012.

[25] "CEB-FIP Model Code," 1990.